

## LETTERS

### Delocalizing Electrons in Water with Light

Dong Hee Son, Patanjali Kambhampati, Tak W. Kee, and Paul F. Barbara\*

Department of Chemistry and Biochemistry, The University of Texas, Austin, Texas 78712

Received: June 26, 2001

Experimental information on the spatial extent of the putative p and conduction band states of the hydrated electron ( $e_{eq}$ ) has been obtained by monitoring and controlling the electron/hole spatial separation of a photogenerated  $e_{eq}$ /hole pair using a femtosecond laser pulse sequence. Optical excitation of  $e_{eq}$  with two photons is observed to dramatically alter its spatial distribution and geminate recombination yield with the hole. One-photon excitation, in contrast, has no effect on the spatial distribution. The results strongly confirm theoretical predictions on the size and location of excited states of  $e_{eq}$ .

Experiment and theory have demonstrated that the equilibrated form ( $e_{eq}$ ) of the excess electron in water, i.e., the hydrated electron, is localized, solvated, and trapped in a  $\sim 3$  Å cavity that is surrounded by approximately six ordered water molecules.<sup>1–11</sup> Much less is known about the optically excited states of  $e_{eq}$ . Theory predicts that the lowest excited state has a p-like electron distribution that is localized on the  $< 10$  Å scale.<sup>12</sup> Higher lying states, however, are predicted to be delocalized in analogy to a conduction band.<sup>9,10,12,13</sup> Here, we provide experimental information on the spatial extent of the putative p and conduction band states by monitoring and controlling the electron/hole spatial separation of a photogenerated  $e_{eq}$ /hole pair using a femtosecond laser pulse sequence. Optical excitation of  $e_{eq}$  with two photons is observed to dramatically alter its spatial distribution and reaction yield with the hole, as expected for the conduction band. In contrast, one-photon excitation has no effect on the spatial distribution. The results strongly confirm theoretical predictions on the size and localization of excited states of  $e_{eq}$  and demonstrate that higher lying conduction band states have a  $> 30$  Å radius, encompassing more than one thousand water molecules.

The three-pulse experiments described herein are an elaboration of the traditional two-pulse, photoionization/probe exper-

iment,<sup>3</sup> as outlined in Figure 1. In the two-pulse experiment (Figure 1a), the first pulse is an intense ultraviolet femtosecond pulse which photoionizes water by a multiphoton process.<sup>14,15</sup> Photoionization has been reported to either involve a direct ionization to the conduction band or, alternatively, dissociative ionization of excited states of water.<sup>14</sup> The positively charged hole is initially  $H_2O^+$ . After a period of  $\sim 1$  ps, the system relaxes to an equilibrated  $e_{eq}$ /hole pair with a distribution of separations that depends on the photoionization conditions (wavelength, pulse energy, and pulse duration).<sup>14,16,17</sup> The relaxed hole is in the form of an OH radical and  $H_3O^+$ , which results from ultrafast fragmentation of  $H_2O^+$ .<sup>14</sup> As time evolves, two processes occur: spatial diffusion of the  $e_{eq}$ /hole pair which alters the distribution of  $e_{eq}$ /hole separations,  $r_{e-h}$ , and geminate recombination (reaction of  $e_{eq}$  with the hole). This latter process only occurs for an electron in close proximity with its hole. The fraction of the electrons that have undergone geminate recombination at a particular probing time is a function of the diffusion process and the initial  $r_{e-h}$  distribution. Typically,<sup>3,14,17</sup> a probe pulse in resonance with the near-IR ground-state absorption of  $e_{eq}$  is used to measure, via the optical density (OD), the time dependence of the surviving concentration of  $e_{eq}$ , e.g., see the two-pulse experimental data (red lines) in Figure 2a,b. Such data can be analyzed to characterize the initial  $r_{e-h}$  distribution.

\* To whom correspondence should be addressed. E-mail: p.barbara@mail.utexas.edu.

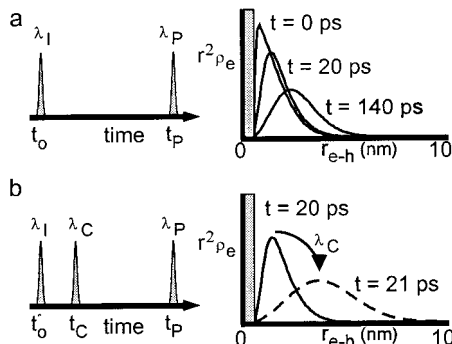
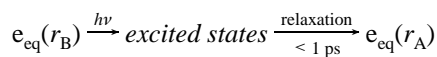


**Figure 1.** Schematic illustration of femtosecond laser based control of the spatial distribution and geminate recombination of the hydrated electron ( $e_{eq}$ ). The sequence consists of an ionization ( $\lambda_I$ ), control ( $\lambda_C$ ), and probe ( $\lambda_P$ ) pulse. In Figure 1a, the ionization pulse produces an initial distribution of excess electrons surrounding the hole which evolves via diffusion and  $e_{eq}$ /hole geminate recombination. In Figure 1b, an additional control pulse spatially redistributes the population of electron far from the hole suppressing the geminate recombination process. The shaded region represents the encounter region where the electron recombines with the hole. The probability distribution function used to describe the initial distribution of  $e_{eq}$ /hole separation is defined as  $\rho_e(r_{e-h}) = (2\pi\sigma_1^2)^{-3/2} \exp[-r_{e-h}^2/2\sigma_1^2]$ , where the average  $e_{eq}$ /hole separation,  $\bar{r}_{e-h}$ , is related to  $\sigma_1$  by  $\bar{r}_{e-h} = 2\sqrt{2}\sigma_1/\sqrt{\pi}$ . The probability distribution function for the migration length of the conduction band electron is defined as  $\rho(l_m) = (2\pi\sigma_2^2)^{-3/2} \exp[-l_m^2/2\sigma_2^2]$ . The average migration length,  $\bar{l}_m$ , is related  $\sigma_2$  by  $\bar{l}_m = 2\sqrt{2}\sigma_2/\sqrt{\pi}$ .

For the three-pulse experiments, a “control” pulse is added to the two-pulse sequence during the evolution period, as outlined in Figure 1. The simulated distributions in Figure 1 represent the actual  $r_{e-h}$  distributions for these experiments. The control pulse is used to prepare short-lived ( $< 1$  ps) excited states of  $e_{eq}$ , as follows:



Here,  $r_B$  and  $r_A$  are the positions of the electron immediately before and after the control pulse. As will be shown shortly, when highly delocalized states are prepared by the control pulse, the  $e_{eq}$ /hole separation,  $r_{e-h}$ , is dramatically increased and the geminate recombination is effectively suppressed by creating this new distribution. The central idea of this experiment is to monitor the effect of the control pulse on the geminate recombination of the electron with its hole and thereby indirectly measure the migration length,  $l_m = r_A - r_B$ , in the photoexcited state.

For the three-pulse data (blue lines in Figure 2a,b), an intense 800 nm femtosecond control pulse is introduced at 20 ps to alter the  $r_{e-h}$  distribution and as a result indirectly affects geminate recombination. Figure 2a,b shows that the control pulse nearly completely suppresses geminate recombination. Of course, when the control pulse is delayed to a later time, i.e., 94 ps in Figure 2c, the effect of spatial redistribution of  $e_{eq}$  on the geminate recombination kinetics is diminished, as much of the recombination has already occurred and the partners have diffused away. The effect of the control pulse on geminate recombination can be measured with a high signal/noise ratio by modulating the control pulse on and off, while keeping the ionization pulse on (Figure 2d). In these data,  $\Delta OD$  reflects the difference between the OD signal with the control pulse on and off. Following the control pulse, the remaining population that was not redistributed by the control pulse continues to undergo geminate recombination. Figure 2d presents  $\Delta OD$  curves for different control pulse energies including low energy

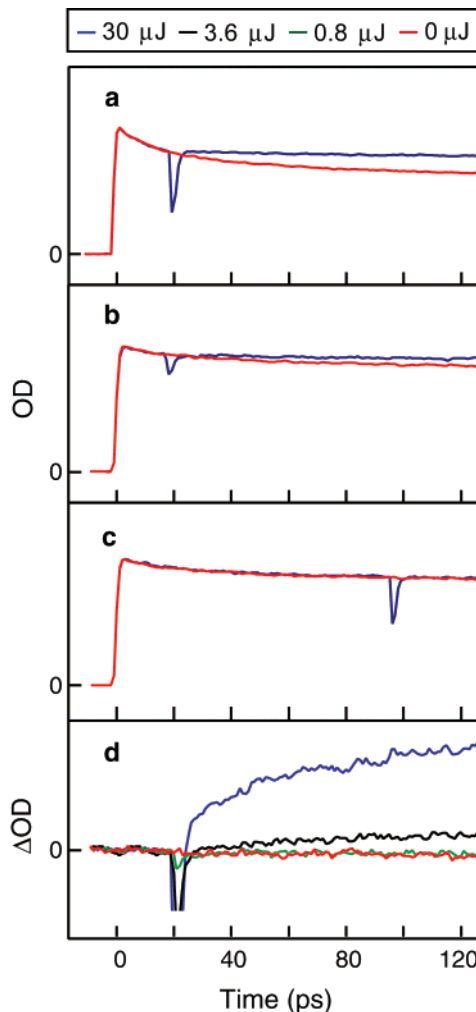


**Figure 2.** Time evolution of the hydrated electron concentration with (red lines) and without (blue lines) control pulse excitation using of 266 (a) and 400 nm (b-d) ionization pulses. The observed geminate recombination dynamics (red lines in a and b) are consistent with those of an earlier work.<sup>14</sup> An analysis of these latter data in terms of the standard classical diffusion/geminate recombination model<sup>16,17</sup> leads to estimates for  $\bar{l}_m$  of 8 and 14 Å with 266 and 400 nm ionization pulse, respectively. The blue lines correspond to three-pulse experiments with 800 nm control pulses arriving at 20 (a, b, and d) and 94 ps (c) after the ionization pulse. The  $\Delta OD$  data in Figure 2d are the difference between the OD signal with the control pulse on and off for alternating pulses. The experiments were performed with an amplified Ti:sapphire laser system producing 35 fs pulses. The fundamental output from the amplifier at 800 nm was either doubled or tripled to produce the 400 or 266 nm photoionization pulses, whereas a portion of the fundamental was used as the control pulse. The remainder of the fundamental was used to generate the probe pulse at 650 nm which was derived from wavelength selected white light continuum. The instrument response was 50 fs (fwhm). The spot sizes/pulse energies at the sample were 100  $\mu$ m/30  $\mu$ J (400 nm) and 5  $\mu$ J (266 nm), 300  $\mu$ m/0–30  $\mu$ J, and 30  $\mu$ m/<1 nJ for the ionization, control, and probe pulse, respectively.

regime for which only a small fraction of the electrons are excited and higher energy regime for which nearly all of the electrons are excited. At very short time-scales (Figure 3) after the control pulse excites  $e_{eq}$ , an absorption bleach is observed because of this  $s \rightarrow p$  excitation (i.e., ground-state depletion). This is followed by rapid repopulation and relaxation of  $e_{eq}$ . Note the time scale of Figure 3 is too short to observe the time-dependence of the  $e_{eq}$  concentration because of geminate recombination and/or suppressed geminate recombination.

We now turn to an assignment of the 800 nm control-pulse excited states that are responsible for the spatial migration of

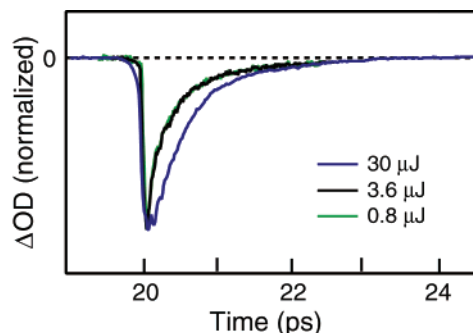


**Figure 3.** Ultrafast spectral relaxation dynamics of the hydrated electron ( $e_{eq}$ ). The relaxation dynamics are independent of the timing of the control pulse. Previous spectroscopic results have demonstrated excitation of  $e_{eq}$  at 800 nm with weak excitation pulses involves a one-photon excitation, which has been assigned to the  $s \rightarrow p$  transition based on a comparison to theory and simulation.<sup>4,5,10,11,18,22,23</sup> After the initial absorption bleach (negative signal) because of  $e_{eq}$  depopulation, the one-photon excited  $p$  state relaxes to repopulate  $e_{eq}$  within a few picoseconds (see the 0.8 and 3.6  $\mu$ J curves). At higher pulse energy (30  $\mu$ J), a previously observed two-photon sequential excitation channel is accessed resulting in slower relaxation dynamics. Because the two-photon channel occurs at an energy at which simulations predict a conduction band, the two-photon prepared state has been assigned to the conduction band from  $s \rightarrow p \rightarrow CB$  sequence.<sup>18</sup>

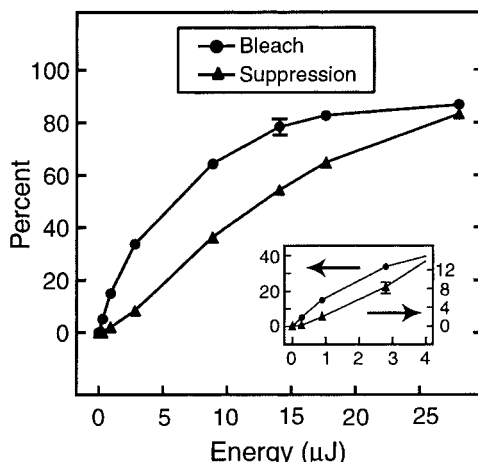


**Figure 4.** Dependence of the absorption-bleach amplitude (circle) and the amount of geminate-suppression (triangle) on the control pulse energy. At high energies, the absorption-bleach amplitude saturates as does the geminate suppression. At low energies (inset), the absorption bleach is linear in pulse energy, whereas the geminate suppression is quadratic. A typical error bar for the geminate-suppression data is shown in the figure inset. The geminate-suppression amplitude is a quantitative measure of the amount of geminate recombination suppressed by the control pulse and defined as  $[\text{OD}\lambda_{C,\text{on}}(t) - \text{OD}\lambda_{C,\text{off}}(t)]/[\text{OD}\lambda_{C,\text{off}}(t_c) - \text{OD}\lambda_{C,\text{off}}(t)]$ , where  $t_c$  is the arrival time of the control pulse ( $\lambda_C$ ). The geminate-suppression curve is identical within the noise of the transients at two different probing times (not shown here) indicating that this experiment resolves suppression without distortion even though the referenced, unsuppressed geminate recombination is not yet complete.

$e_{eq}$ . To demonstrate whether it is the  $p$  or the conduction band (CB) state that suppresses the geminate recombination, a control pulse energy dependence study was undertaken. Figure 4 compares the dependence of both the amount of initial absorption bleach at  $t = t_c$  and the amount of geminate-suppression on the control pulse energy. At low control pulse energies, a small fraction of the  $e_{eq}$  population is excited and the absorption bleach varies linearly with pulse energy, see inset in Figure 4. In this range, the geminate-suppression varies quadratically as a function of pulse energy indicating a two-photon  $s \rightarrow p \rightarrow CB$  transition.<sup>18</sup> At high pulse energies, both the  $s \rightarrow p$  →

absorption bleach and the geminate suppression exhibit saturation because of substantial  $s$  state depletion.

A theoretical model for the time dependent electron survival probability at a given initial and evolving  $e_{eq}$ /hole separation,  $r_{e-h}$ , is well established.<sup>16,17</sup> The model is based on a classical diffusion treatment for the evolution of the  $r_{e-h}$  distribution. We have modified the model to simulate the effect of the control pulse, by convoluting a portion of the diffused  $r_{e-h}$  distribution with a Gaussian radial distribution function that represents the distribution of migration lengths,  $l_m$ , of the excited electron in the one- and two-photon prepared states. Fitting the three-pulse data to the classical diffusion model for  $r_{e-h}$  distribution produces no evidence for spatial migration of the  $p$  state within experimental error and sets an upper limit of 3 Å to the mean migration length,  $\bar{l}_m$ , for the  $p$  state. This result indicates that the  $p$  state is trapped at the same solvent site that was occupied by the original  $s$  state ( $e_{eq}$ ) and that the  $p$  state relaxes to an  $s$  state that is also trapped in the same location. In contrast, the two-photon contribution to the geminate-suppression data clearly reveals electron migration, setting a lower limit on its  $\bar{l}_m$  of 30 Å for the two-photon prepared state. Thus, the previous theoretical assignment<sup>12</sup> of states in this energy range (two photon of 800 nm) to conduction band states is supported by these experiments.

Interestingly, the mean migration length of CB electrons reported herein ( $\bar{l}_m \geq 30$  Å) is significantly larger than initial mean  $e_{eq}$ /hole separation ( $\bar{r}_{e-h} = 8$  Å) for the near-threshold photoionization of water with two photons of 266 nm light, see Figure 2. This is consistent with the previous proposal that the near-threshold photoionization process involves a significant component of local electronic excitation of water and preionization, rather than “pure” excitation to the conduction band.<sup>14,15,17</sup> In contrast,  $\bar{l}_m \geq 30$  Å for the CB electrons is similar to experimental values for the mean  $e_{eq}$ /hole separation ( $\bar{r}_{e-h} \approx 40$  Å) of the related CB electrons produced in the pulsed radiolysis of water.<sup>19</sup> Both values are close to the theoretical estimate for the mean distance between preexisting sites in liquid water<sup>20</sup> that have an appropriate configuration to trap an excess electron without any structural arrangement. This suggests a physical picture for the two-photon  $s \rightarrow p \rightarrow CB$  detrapping process. The femtosecond control pulse apparently creates a compact electron wave packet in the conduction band because of the “bound-to-continuum”  $s \rightarrow p \rightarrow CB$  ultrafast transition. As a result of the excess energy in the conduction band due to the optical transition, the wave packet moves “ballistically” toward the dilute preexisting traps. An excess energy of only 50 cm<sup>-1</sup> would be sufficient to move the electrons to the traps in 50 fs if the effective mass of the CB electron is close to its rest mass.

It is interesting to compare  $\bar{l}_m \geq 30$  Å for the ballistic motion of the CB electrons to the predicted diffusion length for an  $s$  state electron in the same time period (50–150 fs). The  $s$  state would only diffuse 0.4–0.6 Å. Indeed, a localized/trapped electron in any state would be expected to diffuse a similarly short distance because trapping involves a local cavity in the solvent. Trapping dramatically increases the effective mass of the electron because the cavity surrounding the trapped electron must rearrange for the electron to diffuse.<sup>15</sup> The descriptions of quantum delocalization typically employ size criteria such as the radius of gyration or occupancy.<sup>20</sup> The results reported here show that an excess electron in liquid water has a detrapped two-photon 800 nm excited state with a large migration length consistent with the theoretical descriptions of a conduction band, because the electron trapping site is remote from its site of  $e_{eq}$ .

origin. In contrast, the results herein demonstrate that the one-photon 800 nm excited p state of the hydrated electron is trapped and localized at its site of origin. In a separate report, we demonstrate that 400 nm one-photon excitation of the hydrated electron leads to detrapping in analogy to the two-photon 800 nm excitation reported herein.<sup>21</sup>

**Acknowledgment.** We gratefully acknowledge support of this research by the Basic Energy Sciences Program of the Department of Energy and the Robert A. Welch Foundation. We also acknowledge P. J. Rossky, S. M. Pimblott, and D. M. Bartels for helpful discussions.

## References and Notes

- (1) Wiesenfeld, J. M.; Ippen, E. P. *Chem. Phys. Lett.* **1980**, *73*, 47.
- (2) Kenney-Wallace, G. A.; Jonah, C. D. *J. Phys. Chem.* **1982**, *86*, 2572.
- (3) Long, F. H.; Lu, H.; Eisenthal, K. B. *Phys. Rev. Lett.* **1990**, *64*, 1469.
- (4) Silva, C.; Walhout, P. K.; Yokoyama, K.; Barbara, P. F. *Phys. Rev. Lett.* **1998**, *80*, 1086.
- (5) Rossky, P. J.; Simon, J. D. *Nature* **1994**, *370*, 263.
- (6) Emde, M. F.; Baltuska, A.; Kummrow, A.; Pshenichnikov, M. S.; Wiersma, D. A. *Phys. Rev. Lett.* **1998**, *80*, 4645.
- (7) Assel, M.; Laenen, R.; Laubereau, A. *J. Phys. Chem. A* **1998**, *102*, 2256.
- (8) Kloepfer, J. A.; Vilchiz, V. H.; Lenchikov, V. A.; Germaine, A. C.; Bradforth, S. E. *J. Chem. Phys.* **2000**, *113*, 6288.
- (9) Barnett, R. B.; Landman, U.; Nitzan, A. *J. Chem. Phys.* **1989**, *90*, 4413.
- (10) Staib, A.; Borgis, D. *J. Chem. Phys.* **1995**, *103*, 2642.
- (11) Prezhdo, O. V.; Rossky, P. J. *J. Phys. Chem.* **1996**, *100*, 17094.
- (12) Schnitker, J.; Motakabbir, K.; Rossky, P. J.; Friesner, R. *Phys. Rev. Lett.* **1988**, *90*, 456.
- (13) Murphrey, T. H.; Rossky, P. J. *J. Chem. Phys.* **1993**, *99*, 515.
- (14) Crowell, R. A.; Bartels, D. M. *J. Phys. Chem.* **1996**, *100*, 17940.
- (15) Coe, J. V.; Earhart, A. D.; Cohen, M. H.; Hoffman, G. J.; Sarkas, H. W.; Bowen, K. H. *J. Chem. Phys.* **1997**, *107*, 6023.
- (16) Pimblott, S. M. *J. Phys. Chem.* **1991**, *95*, 6946.
- (17) Goulet, T.; Jay-Gerin, J. P. *J. Chem. Phys.* **1992**, *96*, 5076.
- (18) Yokoyama, K.; Silva, C.; Son, D. H.; Walhout, P. K.; Barbara, P. F. *J. Phys. Chem. A* **1998**, *102*, 6957.
- (19) Pimblott, S. M.; LaVerne, J. A. *J. Phys. Chem. A* **1997**, *101*, 5828.
- (20) Motakabbir, K. A.; Schnitker, J.; Rossky, P. J. *J. Chem. Phys.* **1992**, *97*, 2055.
- (21) Son, D. H.; Kambhampati, P.; Kee, T. W.; Barbara, P. F. *Chem. Phys. Lett.* **2001**, *342*, 571.
- (22) Prezhdo, O. V.; Rossky, P. J. *J. Chem. Phys.* **1997**, *107*, 5863.
- (23) Assel, M.; Laenen, R.; Laubereau, A. *Chem. Phys. Lett.* **2000**, *317*, 13.